

GODDARD GRANT
AM-13 CR
115290
33P

ADVANCED SIMULATION AND ANALYSIS OF A
GEOPOTENTIAL RESEARCH MISSION

SEMI-ANNUAL STATUS REPORT
GRANT NAG5-528

Principal Investigator:

B. E. Schutz
The University of Texas at Austin
Center for Space Research
Austin, Texas 78712
(512) 471-4267

January 1988

(NASA-CR-182355) ADVANCED SIMULATION AND
ANALYSIS OF A GEOPOTENTIAL RESEARCH MISSION
Semiannual Status Report (Texas Univ.)
33 p

CSCL 22A

N88-14108

Unclas

G3/13 0115290

Advanced Simulation and Analysis of a Geopotential Research Mission:
Semi-Annual Report, January 1988

Major Events

1. A presentation of current research efforts pertaining to GRM was made at the American Geophysical Union Fall Meeting in San Francisco on December 11, 1987. The presentation was made during the morning poster session. A copy of the abstract and slides presented at the meeting are enclosed.
2. Recent research efforts have culminated in a Doctoral dissertation by Lisa White and a Master's thesis by Peter Antreasian. Both works were accepted by the University in December 1987. Copies of both documents are attached.
3. GRM simulation 8703 was completed. This simulation includes: 1) the 'true' ephemeris which is based upon a geopotential of degree and order 360, 2) the nominal orbit which satisfies the orbit determination requirements of the satellite-to-satellite tracking (SST) configuration, and 3) the relative range-rate measurements corresponding to both the true and nominal orbits.

Present Research Activities

The initial efforts for the current research year continued the study of simulating the orbits and measurement system for the SST configuration. However, the consensus of the scientific community has recently shifted from an SST configuration to the use of a space borne gradiometer. The emphasis of the current research effort has shifted accordingly. However, much of the work in simulating the true orbits of the SST configuration can be used for the gradiometer configuration. The design orbit for GRM probably will not change with the change in configuration. However, the orbit determination requirements for the gradiometer mission have not been established. Therefore, present research efforts are dedicated to:

1. Producing a set of simulated gradiometer measurements for the mission using the ephemeris of the lead satellite from the SST configuration. The set of true measurements will be available soon to the scientific community. The selection of a nominal ephemeris with the corresponding values of the

gradients has not been established due to the uncertainty in the orbit determination requirements.

2. Understanding what the orbit determination requirements for the mission should be and how they might be satisfied. These studies will include discussions with R. Rummel and O. Colombo.
3. Studying the result of using GPS as a tracking system to satisfy the orbit determination requirements.
4. Developing techniques to recover large geopotential fields using gradiometer measurements.

AN INITIAL SIMULATION OF AN ORBITAL GRADIO-METER MISSION

J. B. Lundberg (Center for Space Research, The University of Texas at Austin, Austin, Texas 78712)
B. E. Schutz, B. D. Tapley, and P. Antreasian

Computer simulations have been performed for an orbital gradiometer mission to assist in the study of high degree and order gravity field recovery. The simulations were conducted for a satellite in a near-circular, frozen orbit at a 160 km altitude using a gravitational field complete to degree and order 360. The mission duration is taken to be 32 days. The simulation provides a set of simulated measurements to assist in the evaluation of techniques developed for the determination of the gravity field. Also, the simulation provides an ephemeris to study available tracking systems to satisfy the orbit determination requirements of the mission.

Acknowledgments. This research was supported under NASA Contract No. NAG5-528.

1. 1987 Fall Meeting
2. SCHU027799
3. Dr. B. E. Schutz
Center for Space Research
The University of Texas at Austin
Austin, TX 78712
(512) 471-4267
4. G
- 5.
6. 0
7. 0%
8. Ms. Susie Y. Thorn
Center for Space Research
The University of Texas at Austin
Austin, TX 78712
9. C

INITIAL SIMULATION OF AN ORBITAL GRADIOMETER MISSION

**J. B. LUNDBERG, B. E. SCHUTZ, B. D. TAPLEY
and P. ANTREASIAN**

**Center for Space Research
The University of Texas at Austin
Austin, Texas 78712**

**Presented at the
American Geophysical Union
Fall 1987 Meeting
San Francisco, California**

December 11, 1987

REVIEW OF SIMULATIONS

Objective: The creation of a simulated data sets:

- for the evaluation of techniques developed for gravity recovery from gravity gradiometer or range-rate measurements
- to study the sensitivity of gravity field solution to measurement and orbit determination errors

SIMULATION STUDIES

1. Creation of ephemerides based on 360×360 geopotential field: Simulation 8703
2. Computation of instantaneous relative range-rate measurements for low-low configuration
3. Computation of integrated, one-way doppler measurements for low-low configuration
4. Computation of gravity gradiometer measurements for a single low-altitude satellite
5. Study of the disturbance compensation mechanism

OUTLINE OF GRM SIMULATION S8703

- 32 sidereal days
- Geopotential field complete to degree and order 360 (Rapp, OSU)

$$GM = 3.9860044 \times 10^5 \text{ km}^3/\text{sec}^2$$

$$a_e = 6378.137 \text{ km}$$

- Constant Earth angular velocity vector
- Tides and luni-solar effects not included
- Nongravitational effects not included
- Nominal ephemeris based upon GEM-10B

COMPUTATION OF EPHEMERIDES

Method

- Encke formulation of the equations of motion
- Class 2, fixed-mesh, multistep algorithm of order 10
- CRAY X/MP-24

Comparison

	S8508	S8703
Stepsize (sec)	5	4
Cost per function evaluation (msec)	8.3	23.6
Run time (hr)	5.6	19.2
Ground track closure after 32 days (km)	~2 km	~2 km

DOPPLER DATA SET TO BE DISTRIBUTED

At four-second intervals:

t time tag

$\Delta \dot{\rho}_{n,i}$ integrated one-way doppler measurements
along the nominal orbit received at satellite
i

$\Delta \dot{\rho}_{s,i}$ integrated one-way doppler measurements
along the simulated orbit received at
satellite i

ε_i pseudo-noise parameter

$(\bar{r}_n, \dot{\bar{r}}_n)_i$ position and velocity vectors of the nominal
orbit for satellite i

Nominal gravity field

True gravity field

GRADIOMETER DATA SET TO BE DISTRIBUTED

At four-second intervals:

t time tag

$(T_n)_{i,j}$ gravity gradient along the nominal orbit
($i = 1:3$; $j = 1:3$)

$(T_s)_{i,j}$ gravity gradient along the true orbit

$(\epsilon)_{i,j}$ set of pseudo-noise parameters

$(\bar{r}_n, \dot{\bar{r}}_n)$ position and velocity vectors of the nominal
orbit for satellite

Nominal gravity field

True gravity field

COORDINATE SYSTEMS

- For Satellite Ephemeris:
 - Earth-fixed cartesian
 - Earth-centered, inertial cartesian (optional)
- For Gradiometer Measurements:
 - Earth-fixed cartesian
 - Earth-fixed, radial-north-east
 - Radial, along-track, cross-track

FIT OF NOMINAL REFERENCE ORBIT TO S8703

- Mission requirements for nominal orbit:

Radial position errors (3σ): 100 m
Along-track position errors (3σ): 300 m
Cross-track position errors (3σ): 100 m

- Fitting GEM-10B ephemeris to S8703 resulted in RMS differences of several kilometers
- To meet mission requirements, gravitational coefficients based upon GEM-10B were adjusted: J_2 , J_3 and two pairs of resonant coefficients at orders 16, 17, 33, 49, 82, 164
- Comparison of the final nominal orbit to S8703

	SAT #1		SAT #2	
Direction	RMS (m)	Max Error (m)	RMS (m)	Max Error (m)
Radial	18	64	18	64
Along-track	61	206	61	209
Cross-track	17	69	17	72

Figure 3.1-a Residuals between true & nominal orbits
for satellite one.

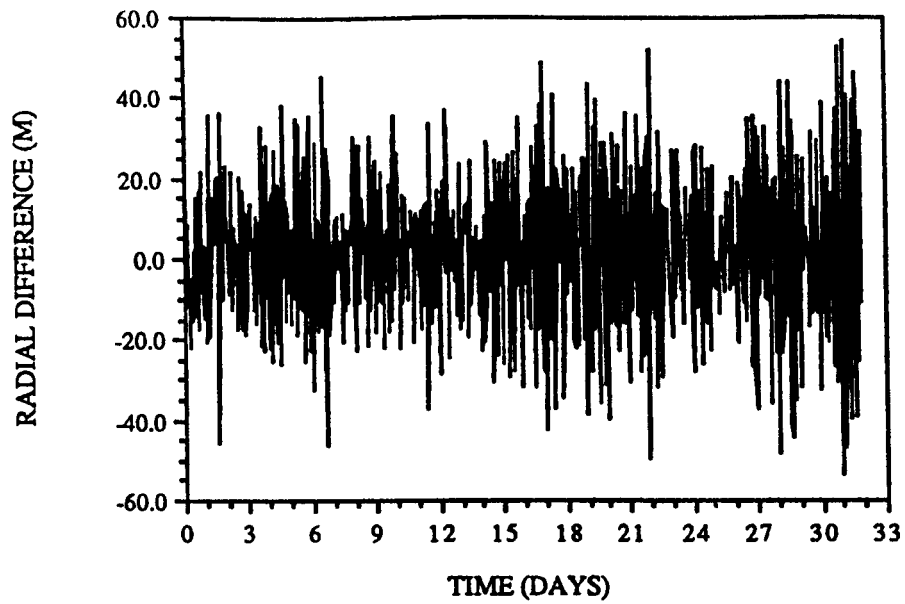


Figure 3.1-b Residuals between true & nominal orbits
for satellite two.

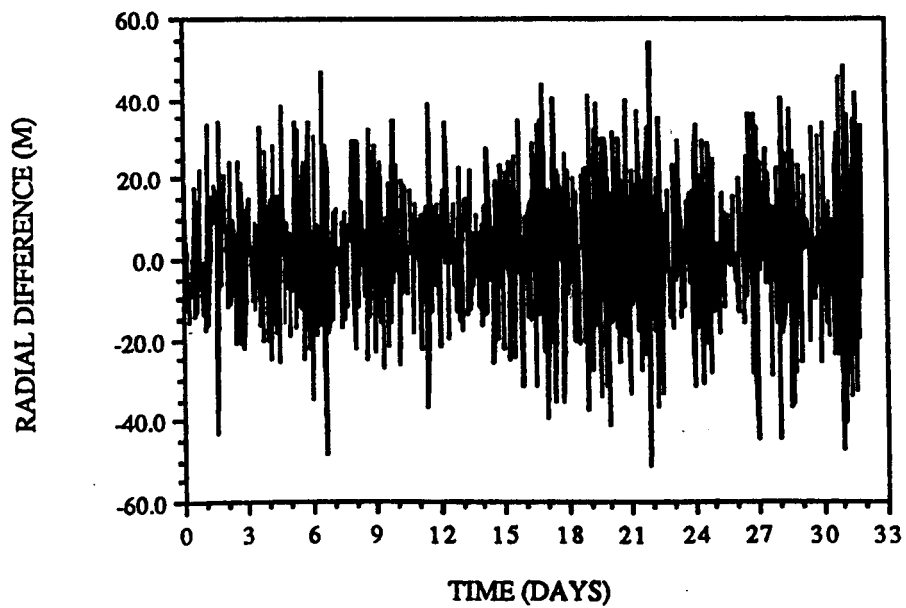


Figure 3.2-b Residuals between true & nominal orbits
for satellite two.

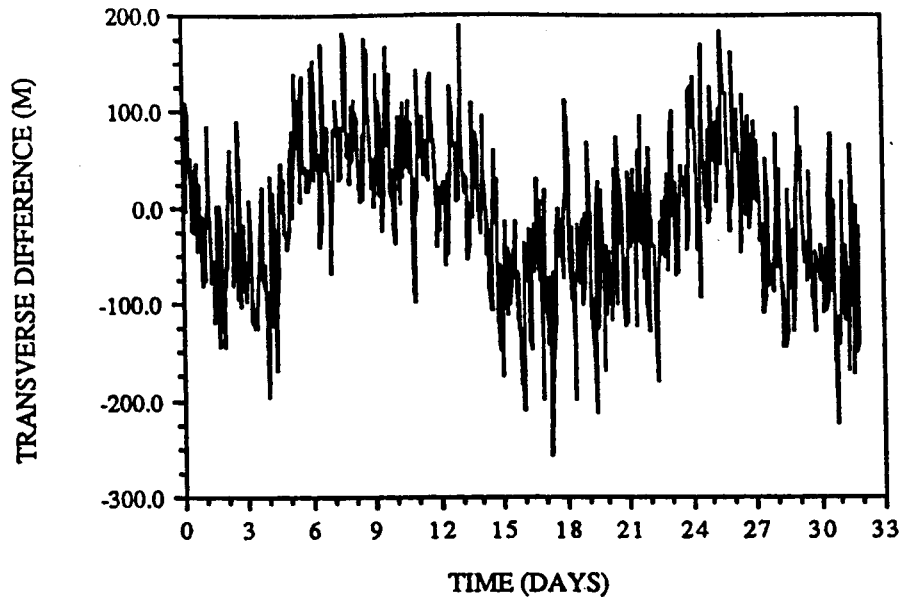


Figure 3.2-a Residuals between true & nominal orbits
for satellite one.

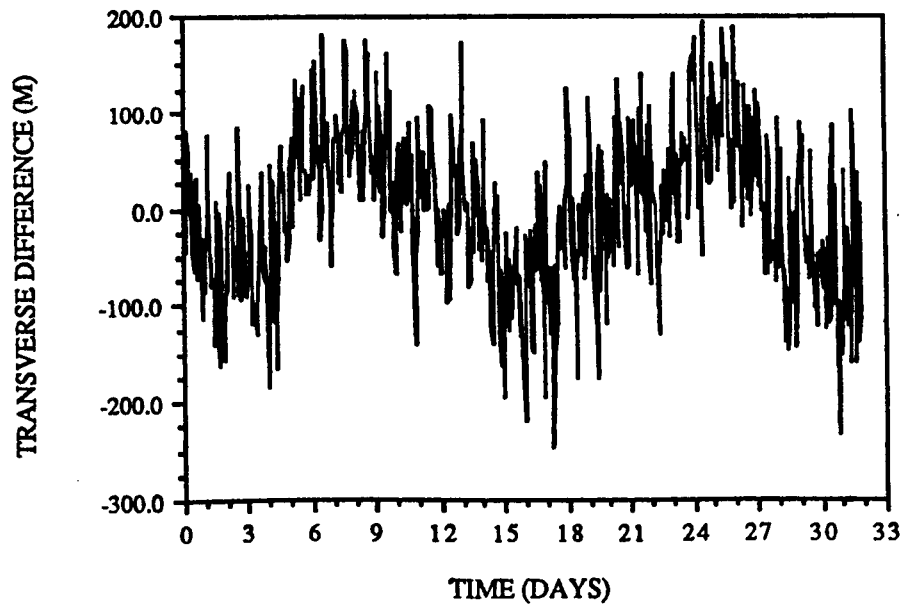


Figure 3.3-a Residuals between true & nominal orbits
for satellite one.

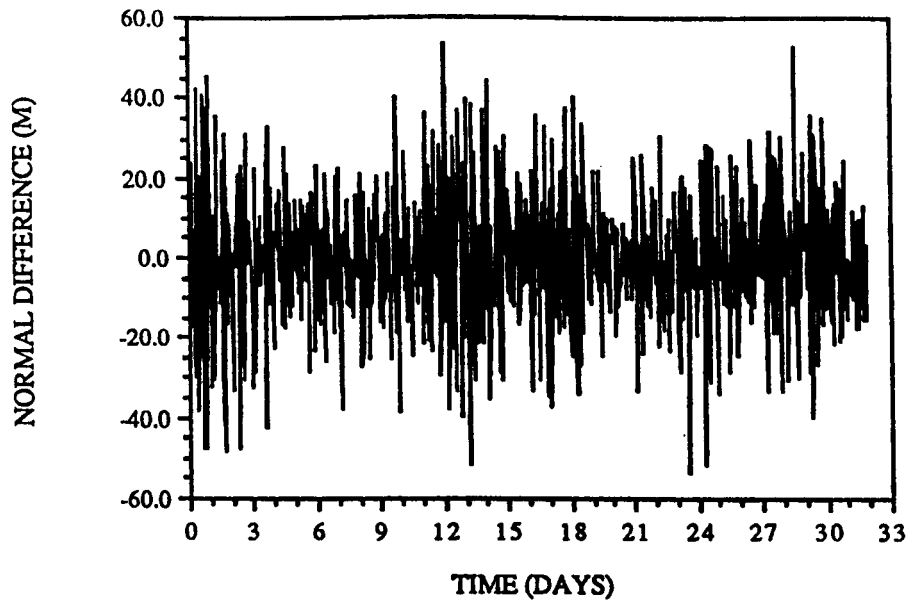


Figure 3.3-b Residuals between true & nominal orbits
for satellite two.

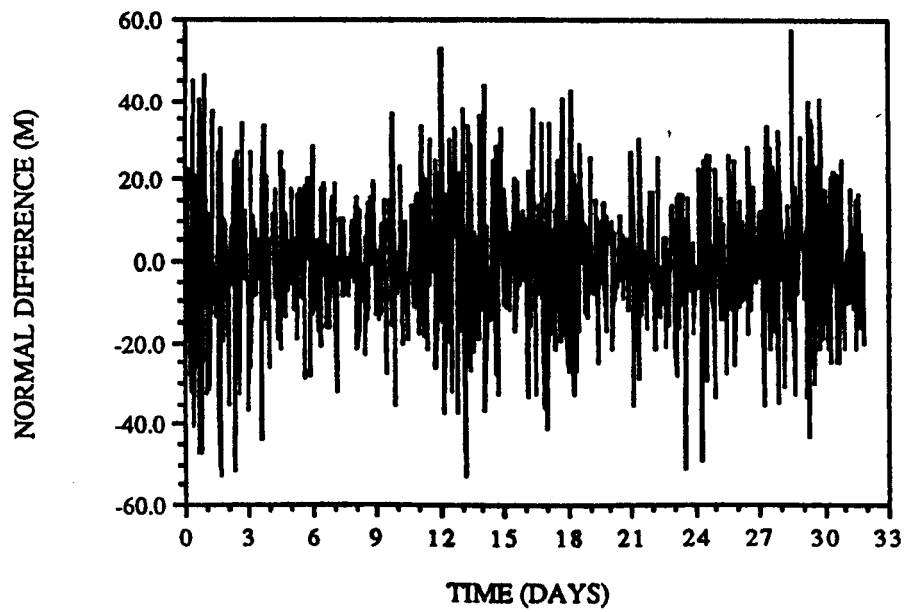


Figure 3.5-a Integrated One-Way Doppler measurements for signal received by
satellite one.

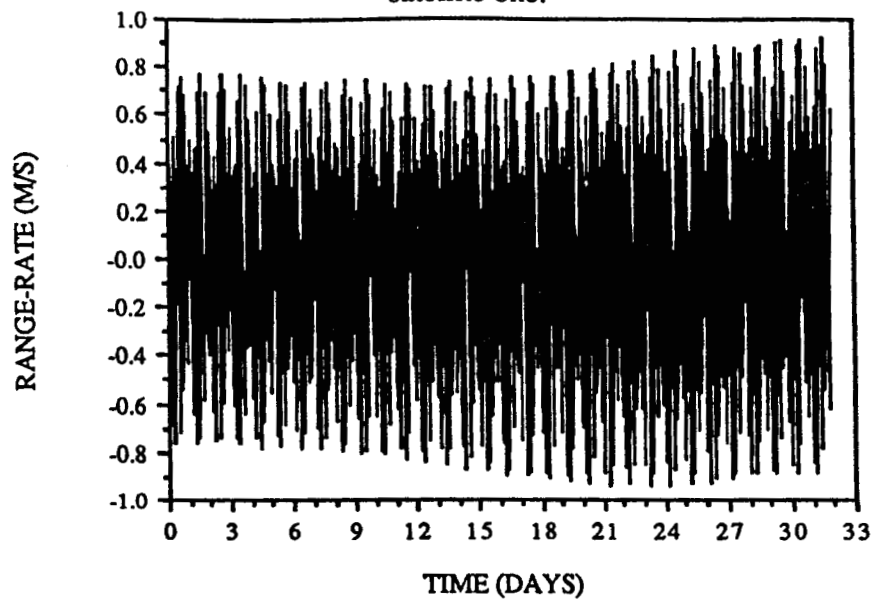


Figure 3.5-b Integrated One-Way Doppler measurements for signal received by
satellite two.

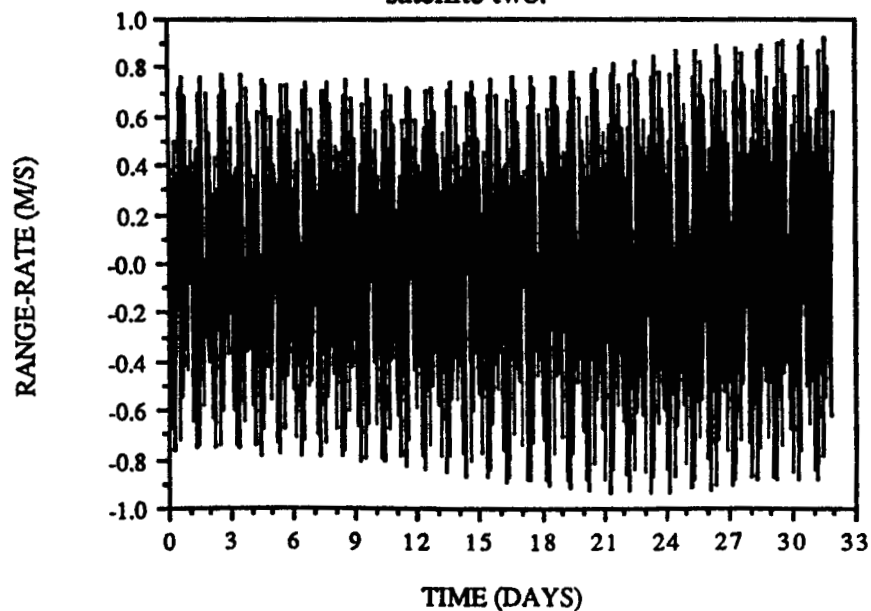


Figure 3.7 Average of both satellite's Integrated One-Way Doppler measurements

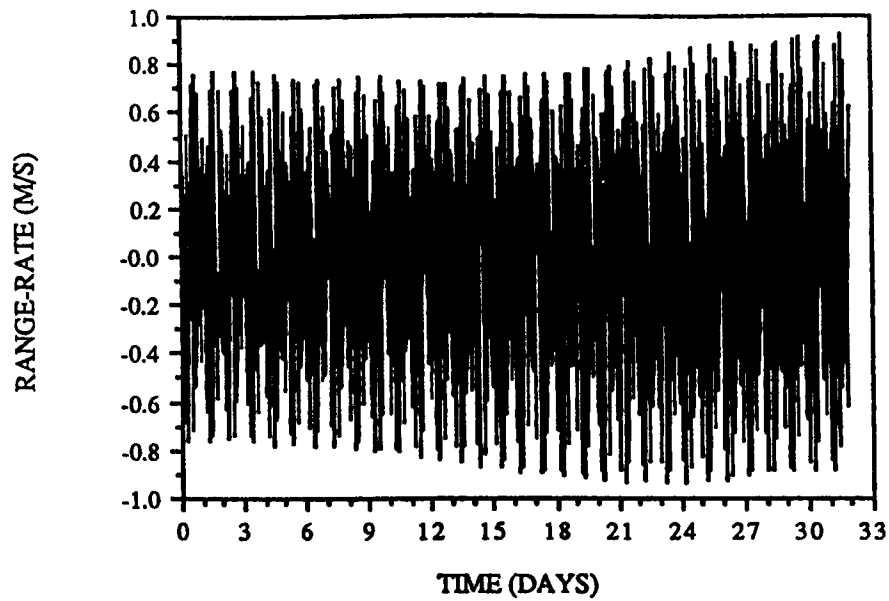


Figure 3.8 The difference between the integrated one-way doppler range-rate measured by satellite 1 and satellite 2.

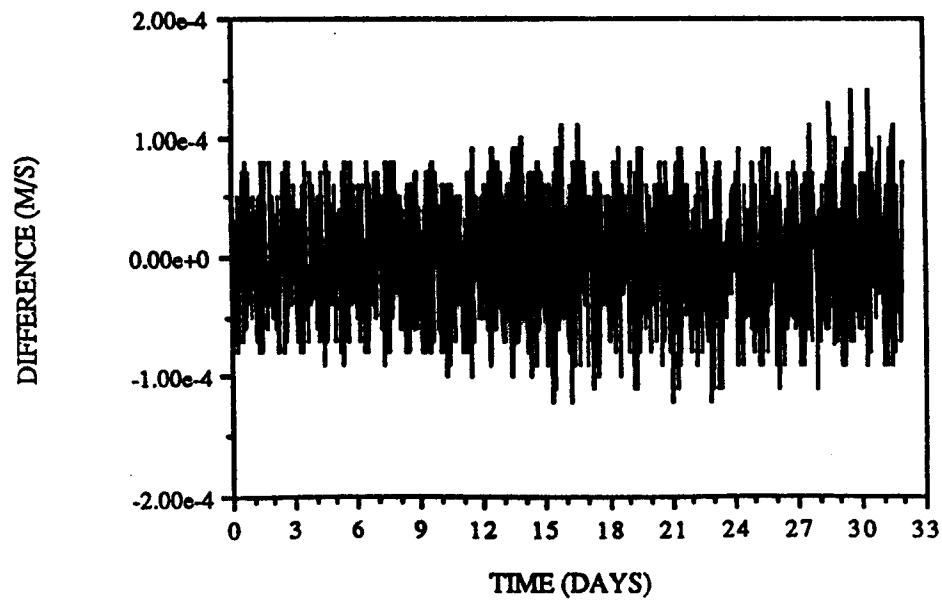


Figure 3.9-a The difference between satellite one and instantaneous range-rates.

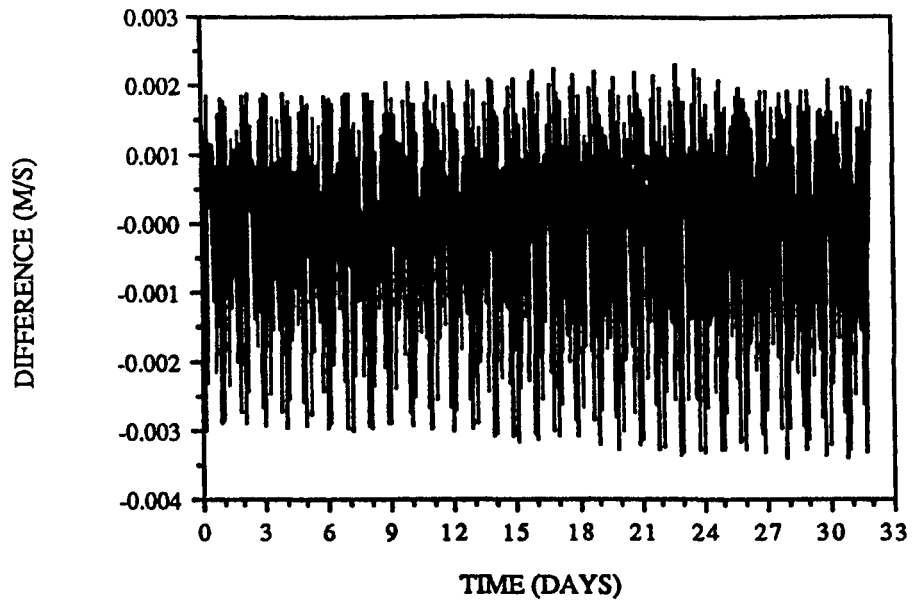


Figure 3.9-b The difference between satellite two and instantaneous range-rates.

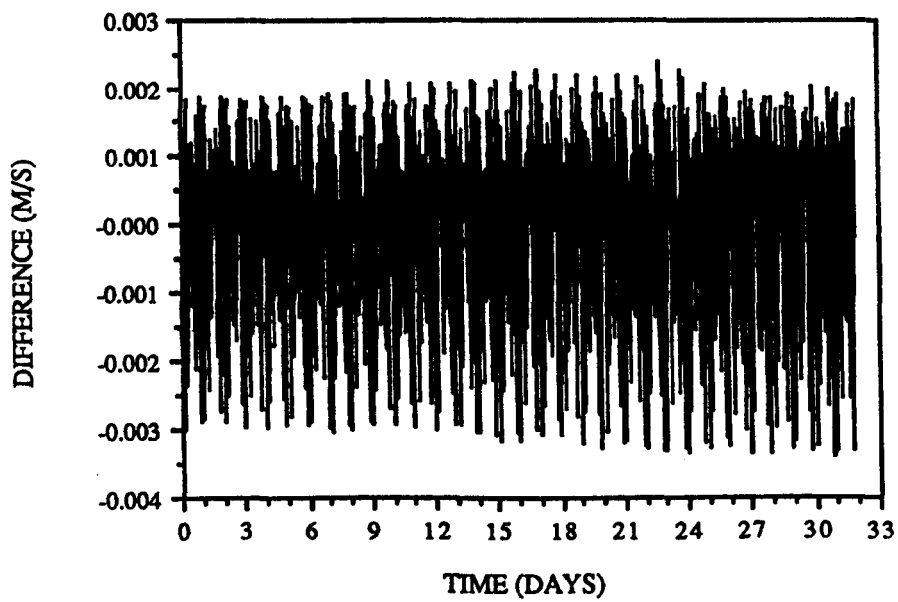


Figure 3.11-a Differences between true & nominal Integrated One-Way
Doppler measurements for satellite one.

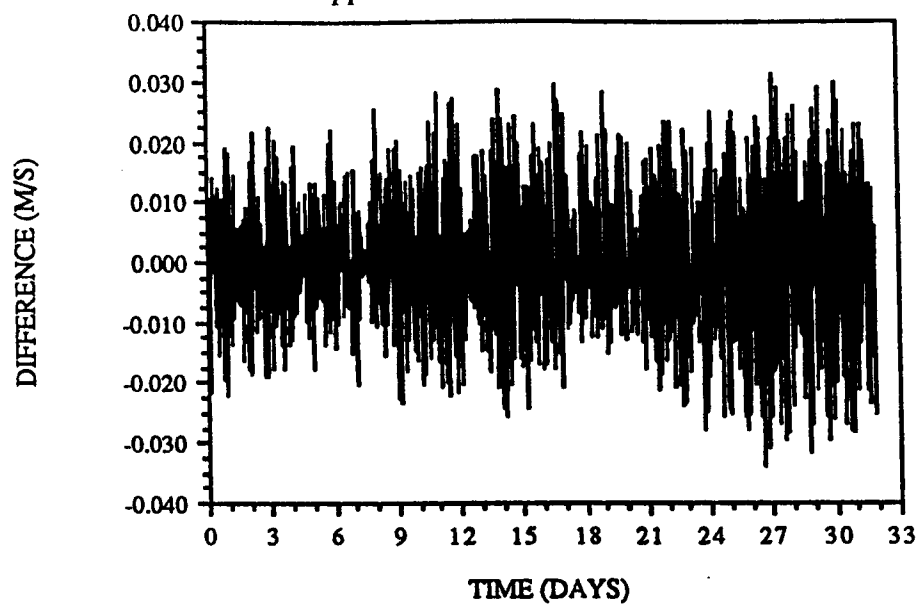
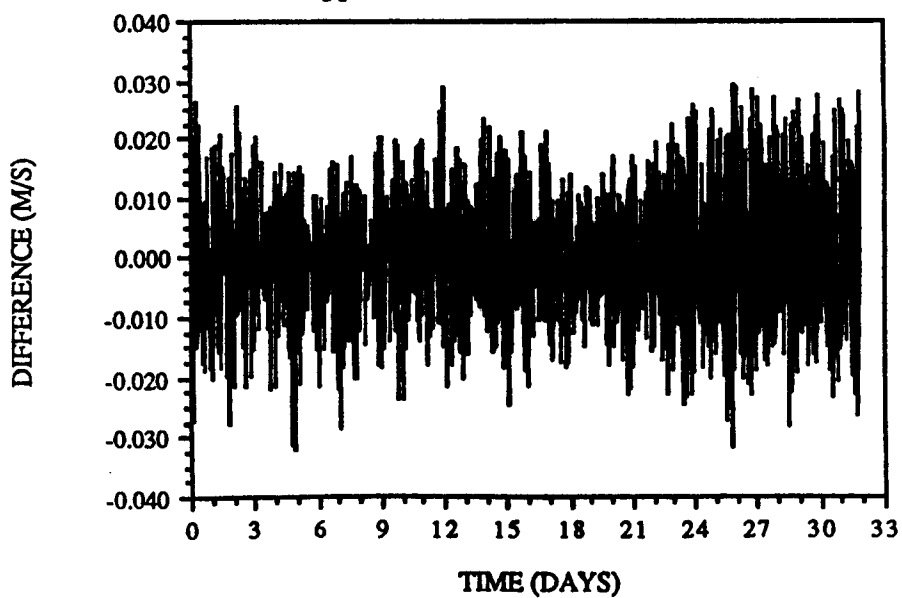


Figure 3.11-b Differences between true & nominal Integrated One-Way
Doppler measurements for satellite two.



PRECEDING PAGE BLANK NOT FILMED

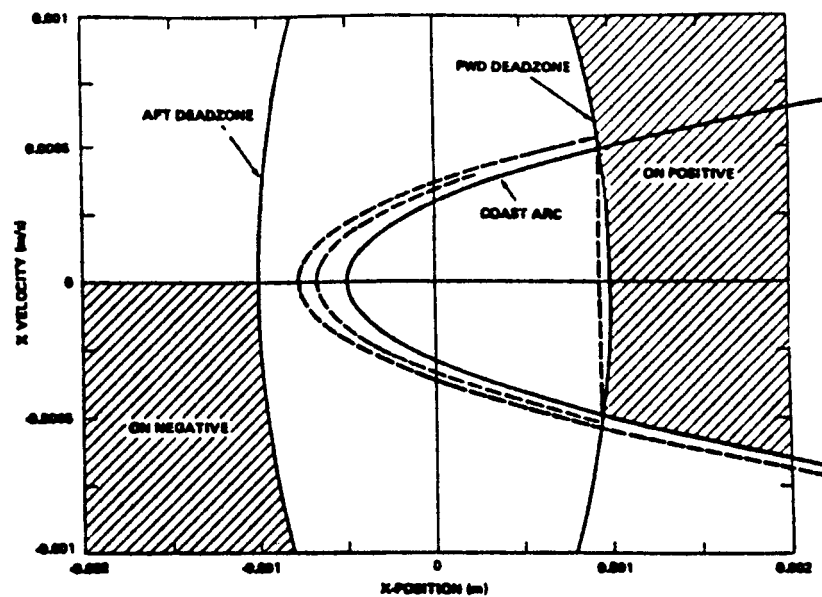


Figure 4.3 Along-track phase plane limit cycle, *Ray & Jenkins*, [1981].

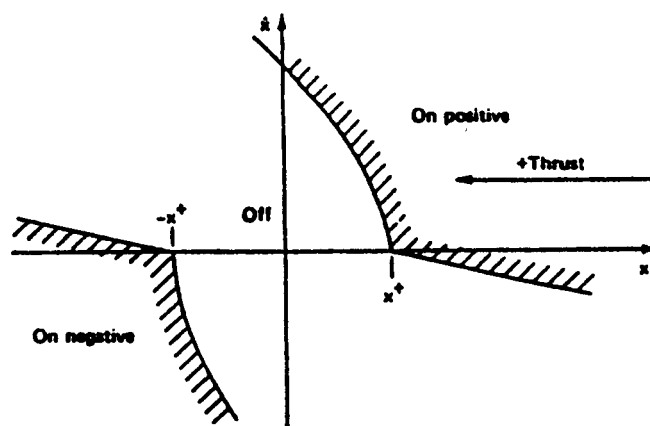


Figure 4.4 Cross-track phase plane limit cycle, *Ray & Jenkins*, [1981].

Figure 4.10 Predicted drag profiles along 2 GRM (160km) orbits on the vernal equinox of 1991 (high solar activity).

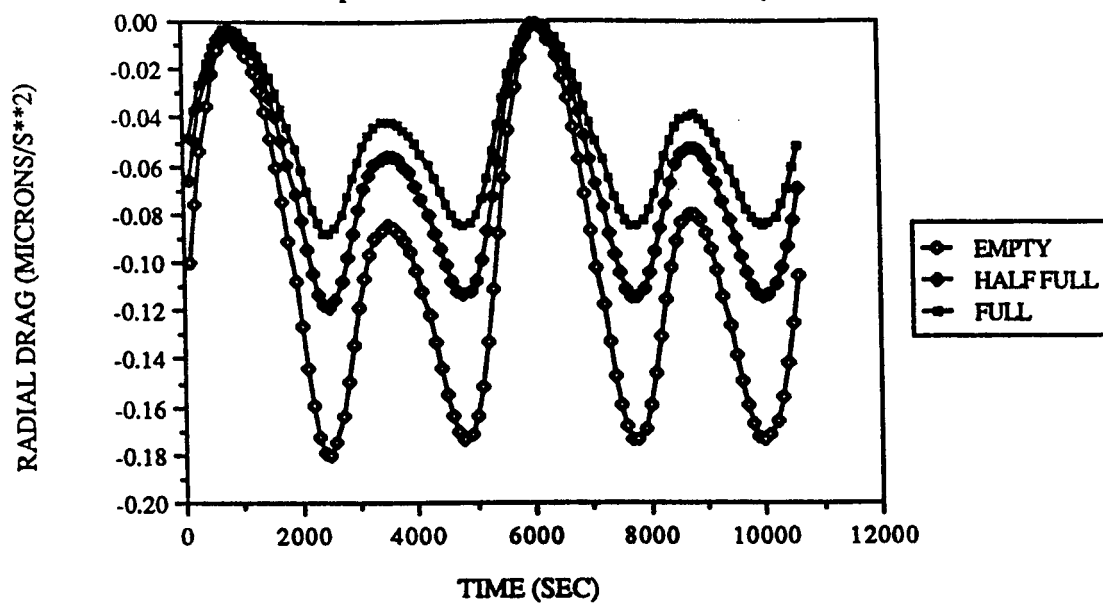


Figure 4.11 Predicted drag profiles along 2 GRM (160km) orbits on the summer solstice of 1996 (low solar activity).

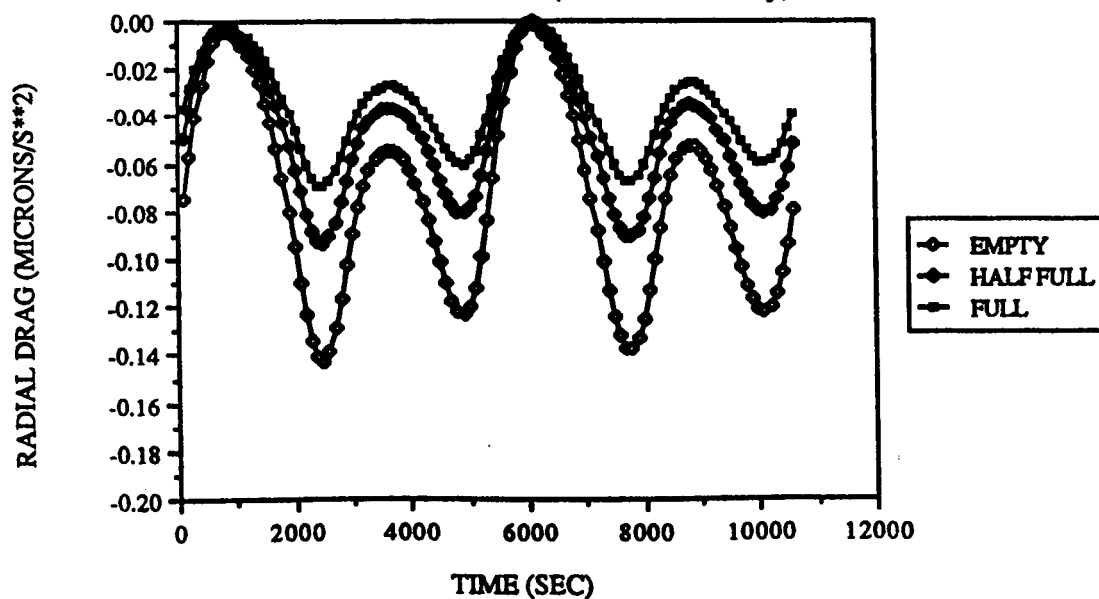


Figure 4.12 Predicted drag profiles along 2 GRM (160km) orbits on the vernal equinox of 1991 (high solar activity).

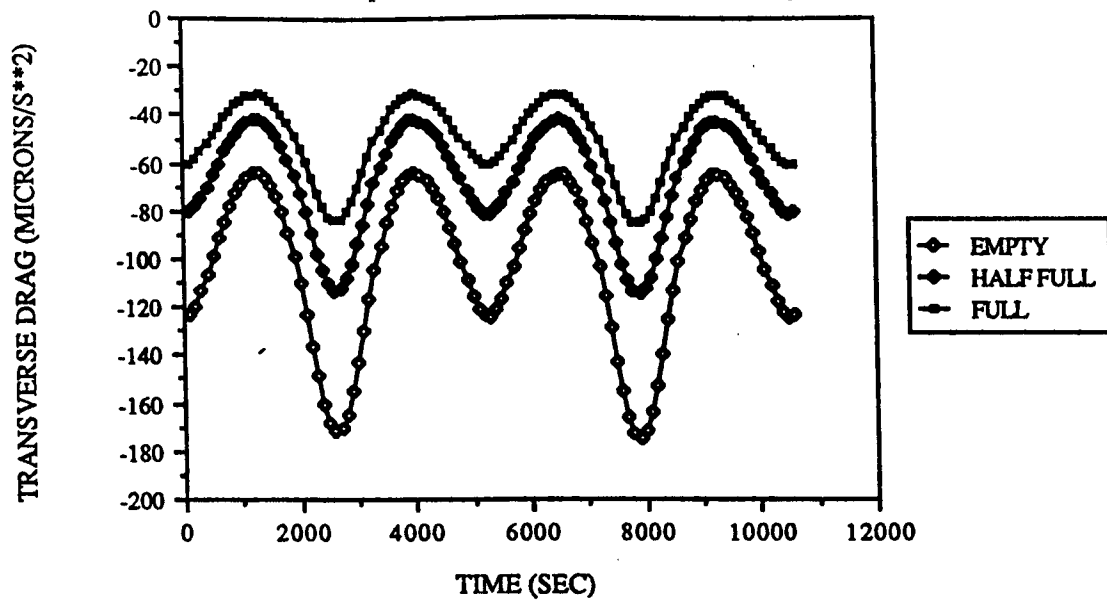


Figure 4.13 Predicted drag profiles along 2 GRM (160km) orbits on the summer solstice of 1996 (low solar activity).

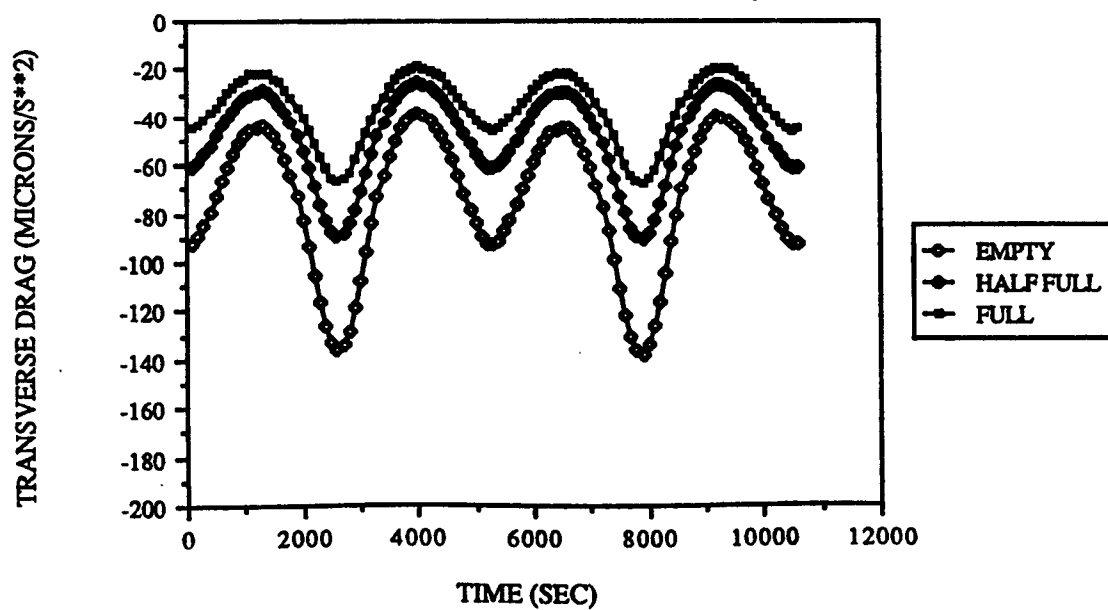


Figure 4.14 Predicted drag profiles along 2 GRM (160km) orbits on the vernal equinox of 1991 (high solar activity).

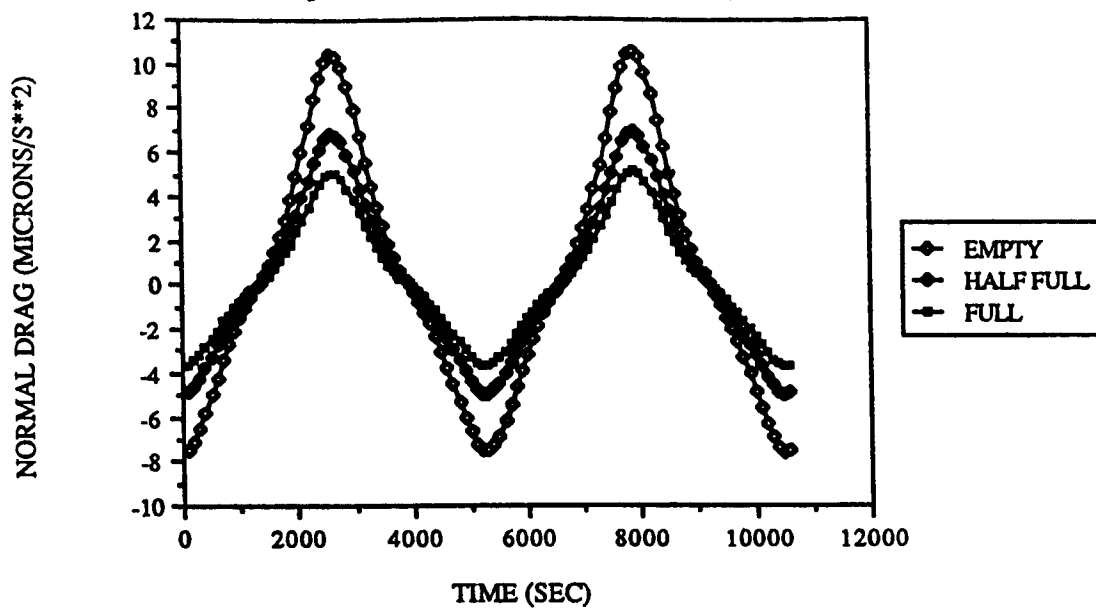
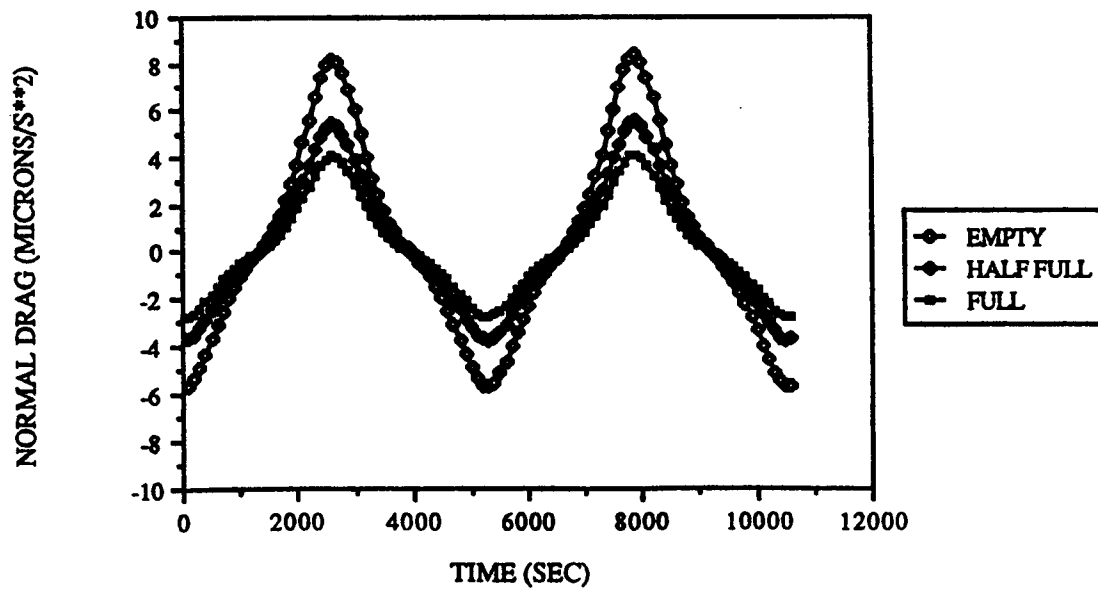


Figure 4.15 Predicted drag profiles along 2 GRM (160km) orbits on the summer solstice of 1996 (low solar activity).



ORIGINAL PAGE IS
OF POOR QUALITY

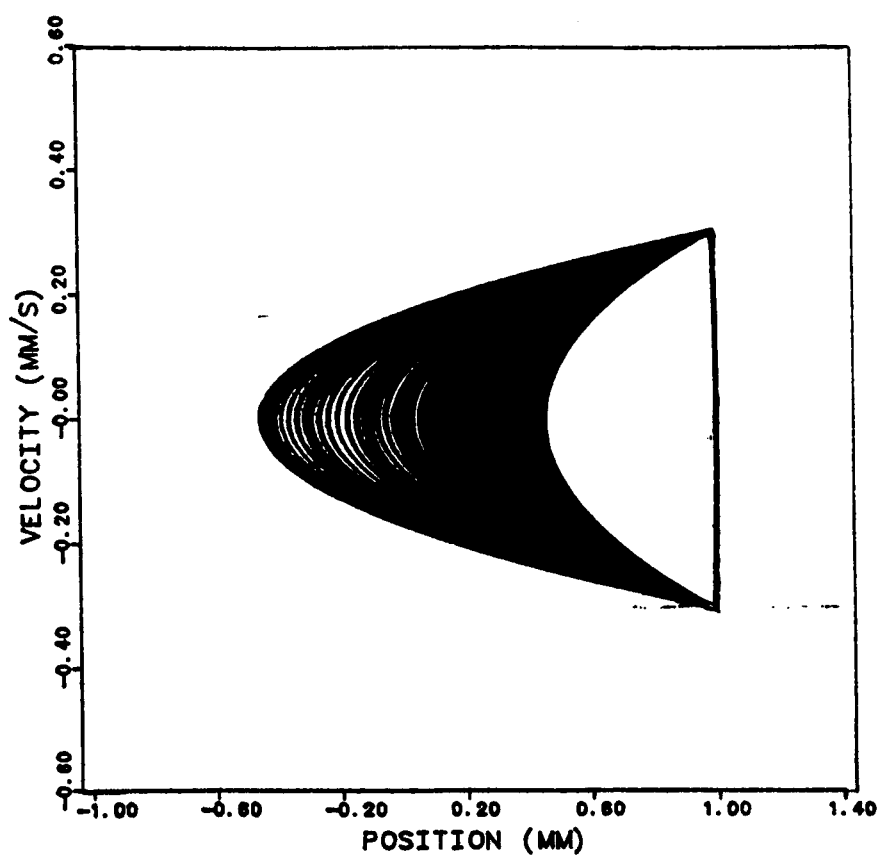


Figure 4.22-a Along-track phase plane limit cycle for one orbit during high solar activity with 95% fuel onboard.

ORIGINAL PAGE IS
OF POOR QUALITY

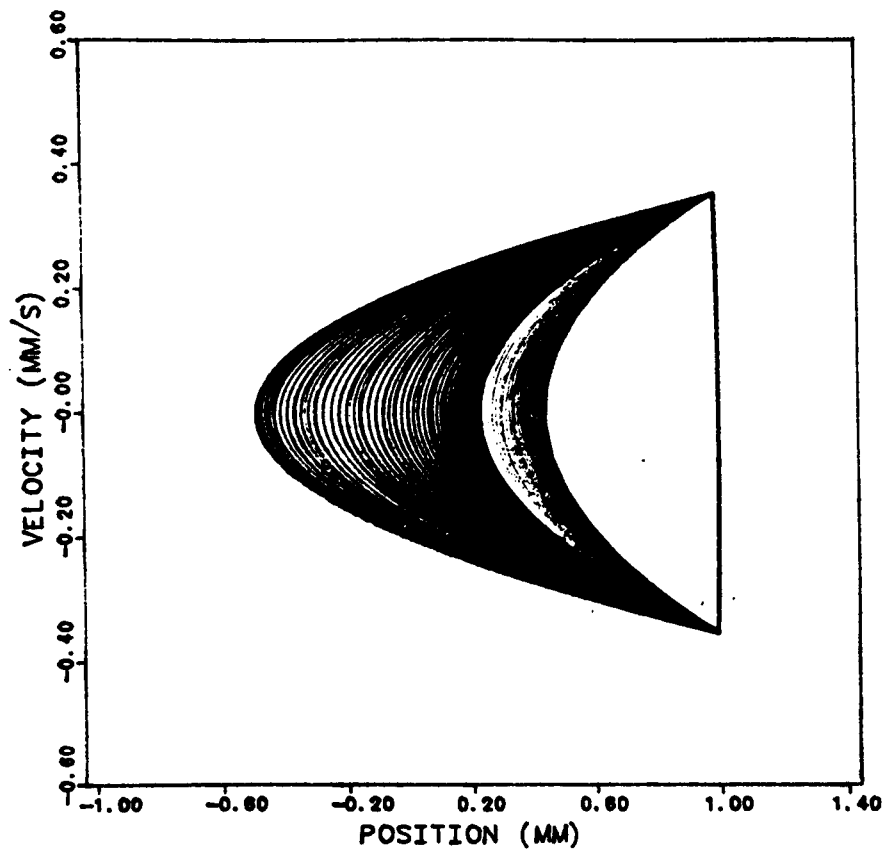


Figure 4.22-b Along-track phase plane limit cycle for one orbit during high solar activity with 50% fuel onboard.

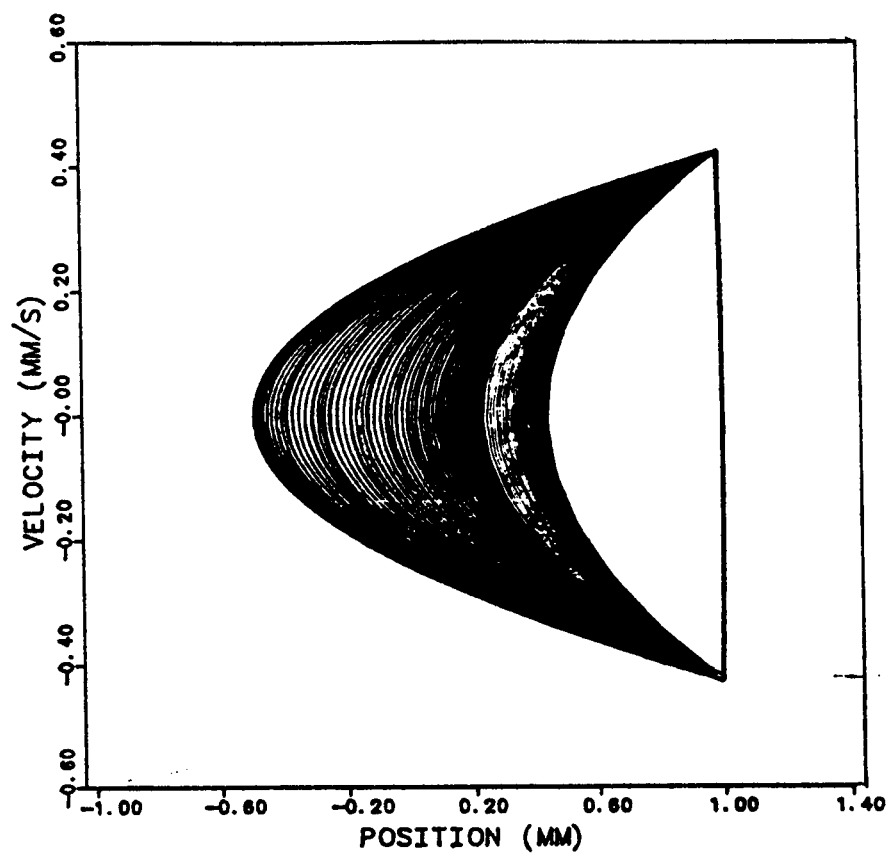


Figure 4.22-c Along-track phase plane limit cycle for one orbit during high solar activity with 5% fuel onboard.

ORIGINAL PAGE IS
OF POOR QUALITY

ORIGINAL PAGE IS
OF POOR QUALITY

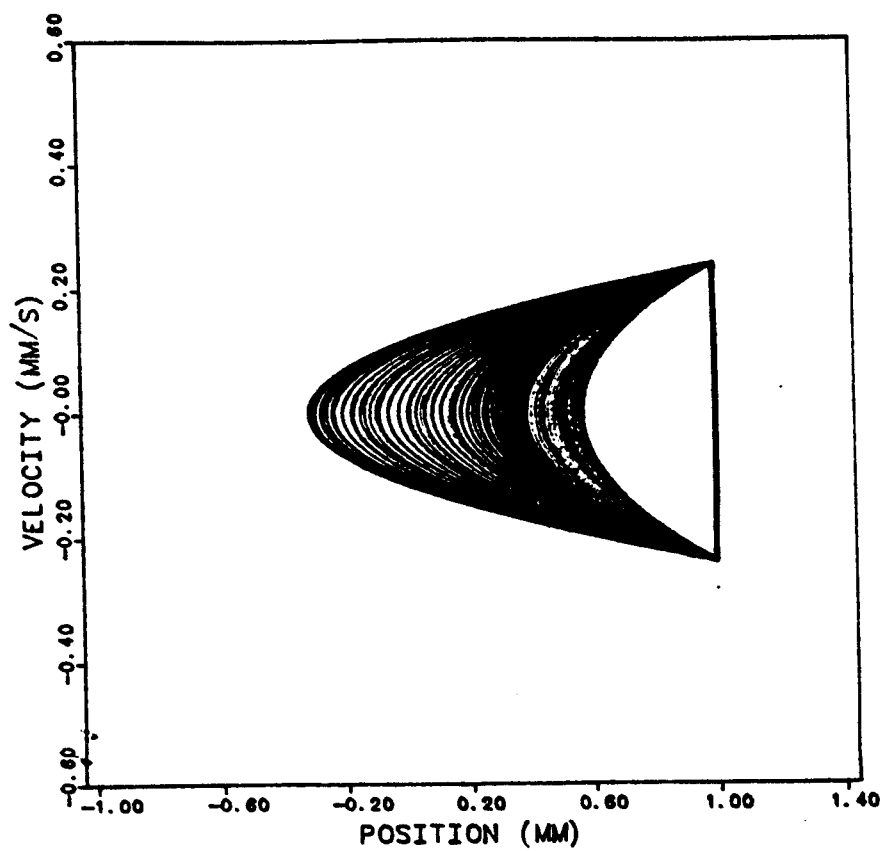


Figure 4.23-a Along-track phase plane limit cycle for one orbit during low solar activity with 95% fuel onboard.

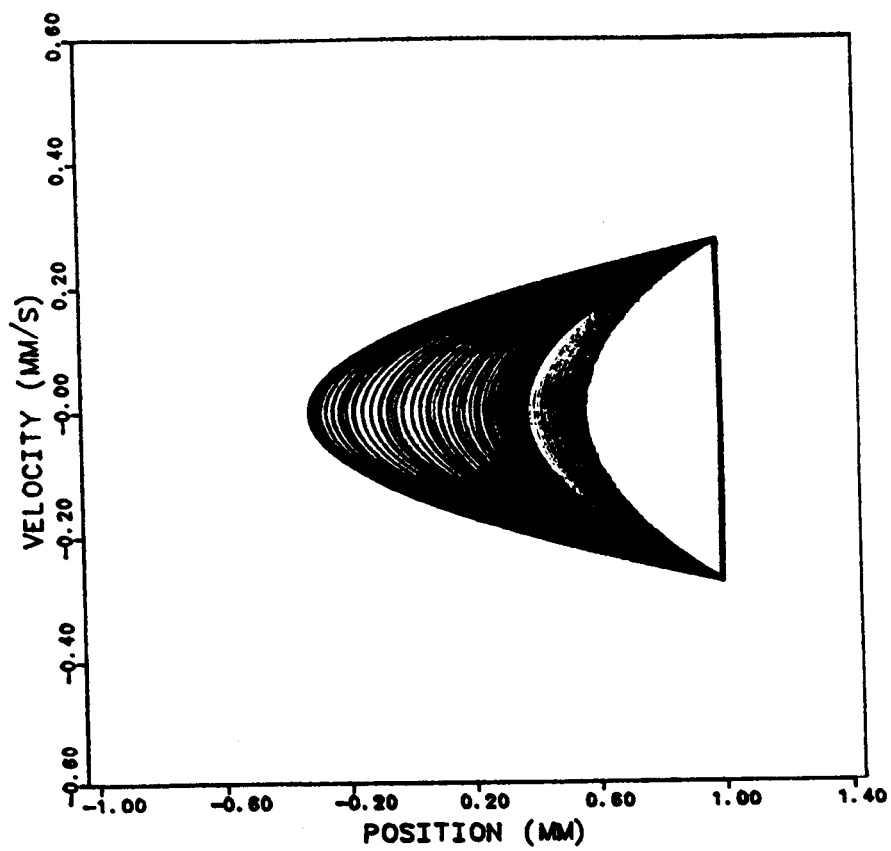


Figure 4.23-b Along-track phase plane limit cycle for one orbit during low solar activity with 50% fuel onboard.

ORIGINAL PAGE IS
OF POOR QUALITY

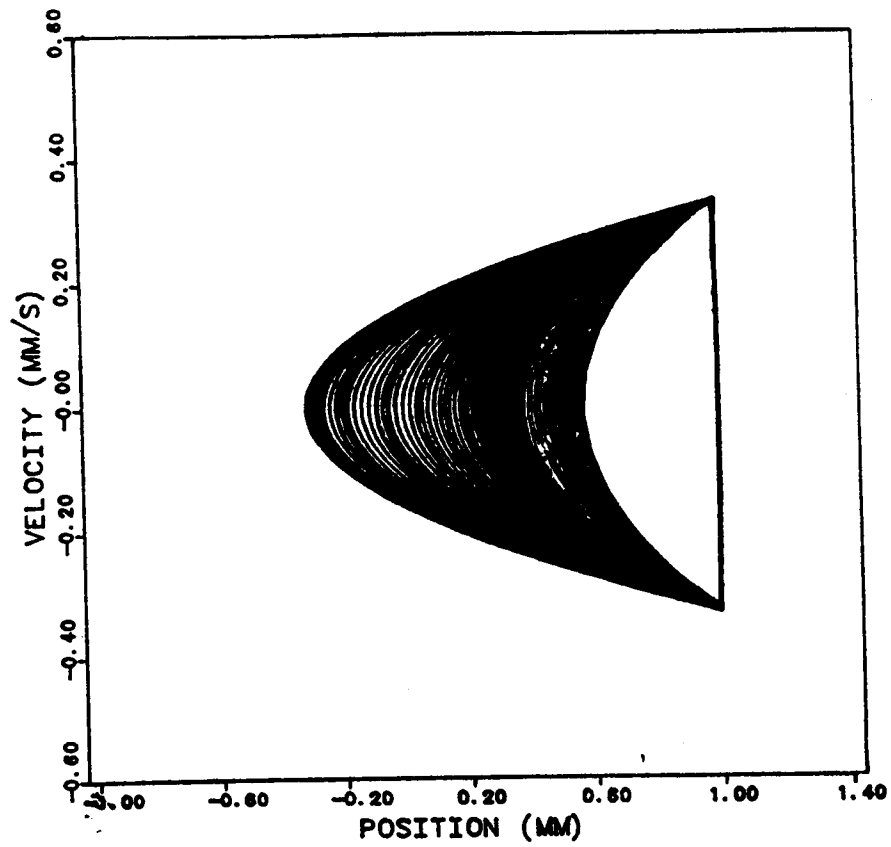


Figure 4.23-c Along-track phase plane limit cycle for one orbit during low solar activity with 5% fuel onboard.

Figure 3.6-a Time of flight of signal received by satellite one.

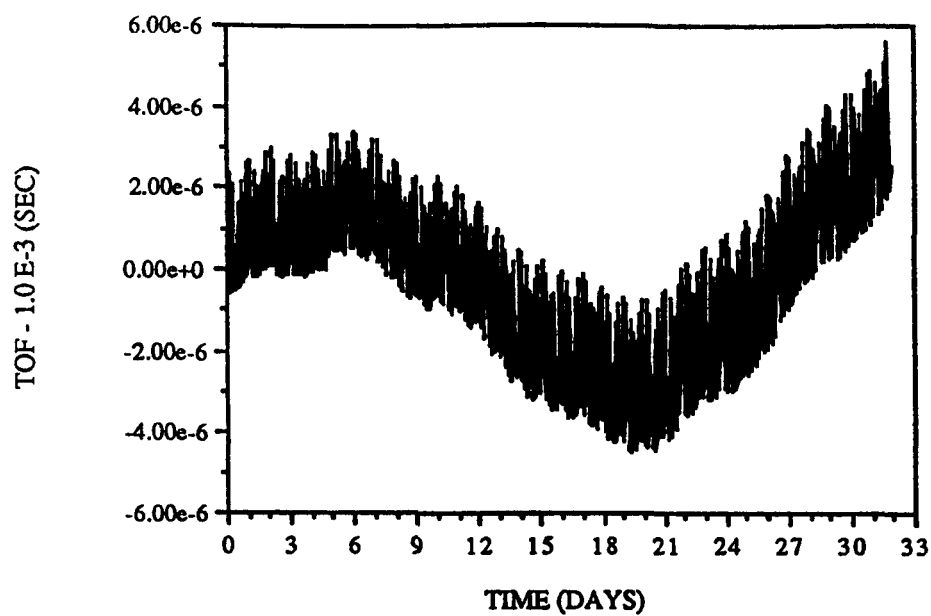


Figure 3.6-b Time of Flight of signal received by satellite two.

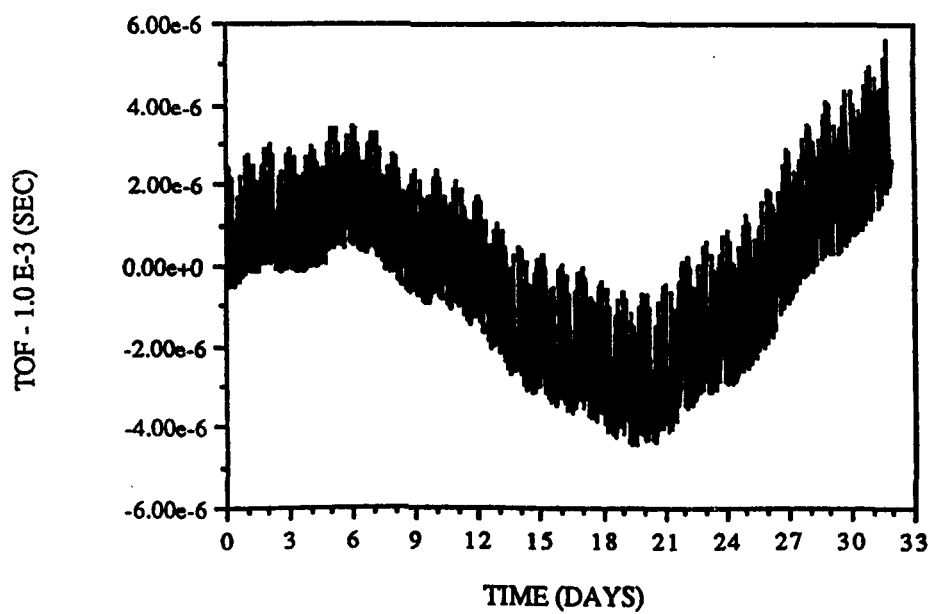


Figure 3.10 The difference between instantaneous and average range-rates.

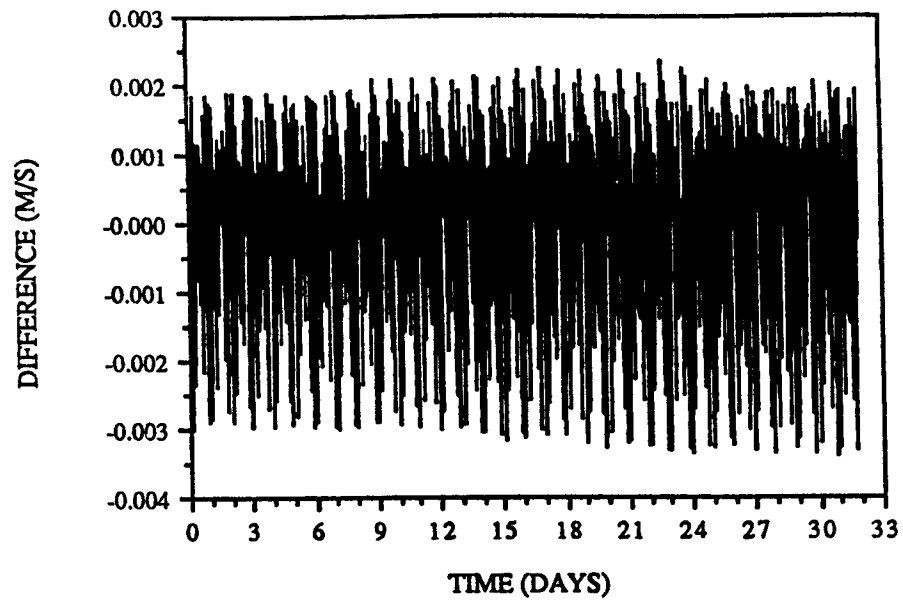


Figure 4.8 Predicted latitudinal atmospheric density variation for the vernal equinox of 1991 at GRM altitudes.

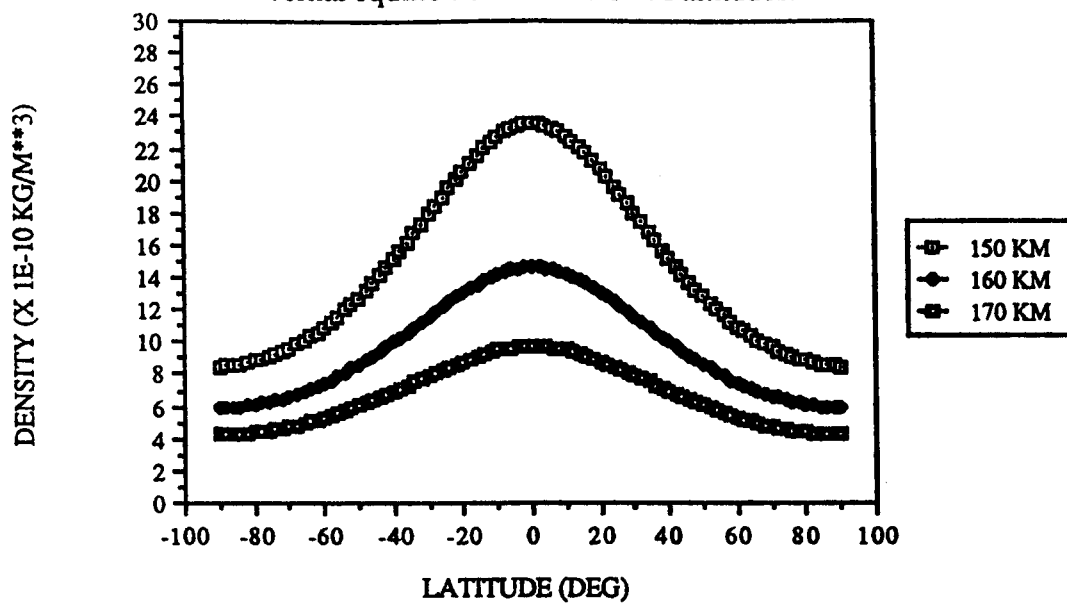


Figure 4.9 Predicted latitudinal atmospheric density variation for the summer solstice of 1996 at GRM altitudes.

